

ANDRZEJ PAWŁOWSKI*, TOMASZ CZEPE*, LESZEK GÓRSKI**

THE PHASE STRUCTURE OF METALLIC AND CERAMIC PLASMA SPRAYED PROTECTIVE COATINGS

STRUKTURA FAZOWA W METALICZNYCH I CERAMICZNYCH WARSTWACH NATRYSKIWANYCH PLAZMOWO

The chemistry and microstructure of ceramic coatings of ZrO_2 with 8 and 20 wt% Y_2O_3 plasma deposited on the NiCrFe substrate with the NiCr25Al6Fe2Y0.4 interlayer were investigated using scanning, analytical microscopy and X-ray phase analysis. An amorphous phase and fine crystalline zone adjacent to the ceramic and metallic layer was detected using transmission electron microscopy. On the other hand, another zone, which was nanocrystalline with some contribution of amorphous phase was observed in the NiCrAlFeY interlayer close to the NiCrFe substrate.

Zaprezentowano wyniki badań struktury warstwy tlenkowej o składzie $ZrO_2 + 8\text{cięż.}\%Y_2O_3$ oraz $ZrO_2 + 20\text{cięż.}\%Y_2O_3$ osadzonej plazmowo na podłożu stopu NiCrFe z warstwą pośrednią NiCr25Al6Fe2Y0.4 wraz z analizą składu i dyfrakcji elektronowej tych warstw. Stosowano techniki: rentgenowskiej analizy fazowej, skaningowej i transmisyjnej mikroskopii elektronowej wraz z analizą składu w nanoobszarach techniką EDS. Stwierdzono obecność amorficznej fazy i drobnokrystalicznego obszaru fazy ceramicznej w sąsiedztwie z warstwą metaliczną oraz obszaru nanokrystalicznego z udziałem fazy amorficznej w nakładanej plazmowo metalicznej warstwie przejściowej NiCrAlFeY, krzepnącej na podłożu NiCrFe.

1. Introduction

Ceramic layers sprayed on a metallic substrate in plasma environment at high temperature form excellent thermal barrier coatings required in high technology instruments like thermal and gas turbines or jet and diesel engines. High temperature of

* INSTYTUT METALURGII I INŻYNIERII MATERIAŁOWEJ IM. ALEKSANDRA KRUPKOWSKIEGO PAN, 30-059 KRAKÓW, UL. REYMONTA 25.

** INSTYTUT ENERGII ATOMOWEJ, 05-400 OTWOCK-ŚWIERK

the plasma arc, of milisechs order, results in a high solidification time of the layer about 10^5 – 10^6 K/s. Such a high solidification time may in turn result in considerable segregation of composition as well as the appearance of non-equilibrium phases [1]. The fine crystalline morphology and amorphous phases produced in such conditions in the plasma sprayed layer are vital parameters, which determine the resistance to rapid changes of temperature and thermal shocks.

Chreska and King [2] have observed the microstructure of a plasma sprayed layer consisted of $ZrO_2 + 6\text{--}8$ wt% Y_2O_3 on the NiCrAlY substrate in a high-resolution transmission microscope. They found a layer built of nanocrystalline and partly amorphous phase between the ceramics and the substrate, while, within the ceramics, columnar crystals of 30–100 nm size were recorded. Bartuli *et al.* [3], analysing the composition of the interlayers produced, registered the increase of aluminium content and traces of yttrium as a result of their diffusion in the liquid state from the substrate. Wołczyński, Kloch and Pawłowski [4] found a layer-like arrangement of grains with variable composition from 6 up to 10 wt% Y_2O_3 . Based on theoretical models of solidification, they suggested different modes of crystallization of grains throughout the subsequent interlayers. Pawłowski, Czeppe and Górski [5] noticed the occurrence of nanocrystalline structure with a contribution of amorphous phase in the metallic transition layer close to the ceramics.

The research was aimed at the determination of structure and grain morphology of the ceramic layers of composition $ZrO_2 + 8\text{wt}\% Y_2O_3$ and $ZrO_2 + 20\text{wt}\% Y_2O_3$ as well as phase morphology of the metallic NiCrAlY interlayer produced as a result of plasma spraying on NiCrFe metallic substrate.

2. Experimental procedure

The ceramic coatings were deposited by the method of Atmospheric Plasma Spraying (APS) with the use of plasmatrone type PN-120 in the Institute of Atomic Energy, Świerk. The ceramic powder of 50–100 μm grain size was produced by the co-precipitation method in the form of ZrO_2 – Y_2O_3 solid solution of cubic symmetry. The powder was introduced into the plasmotrone at ambient temperature and was heated up to 10^4 K during few milisechs, while the cooling rate at the air-cooled substrate was 10^5 – 10^6 K/s. The ceramic layers, 150–200 μm thick, contained 8 and 20 wt% Y_2O_3 and were deposited onto the transition metallic NiCr25A16Fe2Y0.4 layer 50 μm thick, which was also plasma deposited on NiCrFe substrate in order to increase the adherence of the ceramics. Spraying process parameters, experimental details and some properties of the obtained thermal barrier coatings (TBC) were described elsewhere [6, 7, 8].

The measurements of lattice parameters of the phase based on the zirconium dioxide of cubic symmetry as well as the measurements of crystallite size at various distance from the substrate were carried out by an X-ray method on Philips PW 1710 diffractometer using $CoK\alpha$ radiation.

The investigation of microstructure and the composition analysis of the ceramics and transition layers on their cross-sections were performed by the use of scanning electron microscope with Energy Dispersion Spectrometer (EDS) attachment. The analysis of grain morphology and electron diffraction patterns taken of chosen areas of layers were carried out on analytical transmission electron Philips CM20 Twin microscope using ion thinning to prepare thin foils.

3. Results and discussion

3.1. The X-ray phase analysis

The analysis of the ceramic layer performed at different distances from the metallic interlayer showed that a strong maximum 220 from the cubic ZrO_2 -c phase deteriorates as the distance from the surface becomes greater. Simultaneously a weak 211 maximum from the tetragonal ZrO_2 -t increases as the distance to the metallic layer gets smaller [6]. This suggests that there is an influence of solidification rate on the incidence of ZrO_2 phases along the layer cross-section. The calculation of the data collection depth in these conditions showed that the analysed depth was 14 μm , at intervals about 50 μm and ceramic layer thickness from 150–200 μm . The analysis of the lattice parameter based on 220 ZrO_2 -c reflection, as the metallic layer was approached, showed that the a lattice parameter of the solid solution decreased at increasing distance from the substrate, and after it attained a local minimum it started to rise (Fig. 1a). The differences observed results from the segregation of the ceramic grain content due to different cooling rate at solidification. The a -values for the ceramics with 20 wt% Y_2O_3 are slightly lower than for the 8 wt% Y_2O_3 content. The crystallite size, D measured with the X-ray method, was assessed at both contents of Y_2O_3 to increase from 10 up to more than 100 units or even 200 units followed by a local minimum and subsequent increase up to 200 units together with the increasing distance from the substrate (Fig. 1b). The D -values were found to be higher for the ceramics with 8 wt% Y_2O_3 than for the other. The changes correspond to different rates of solidification of subsequent ceramic layers.

3.2. SEM microstructure and chemical composition (EDS) analyses

The observations of microstructure by the SEM method with the chemical analysis using the EDS technique derived, for the two contents of Y_2O_3 analysed, the changes in Y_2O_3 content in solid solution grains due to the variable solidification conditions across the ceramic layer. The larger difference of content between the centre of the grain and its boundary was observed in the 20 wt% Y_2O_3 ceramic than in the 8 wt% Y_2O_3 one (Fig. 2).

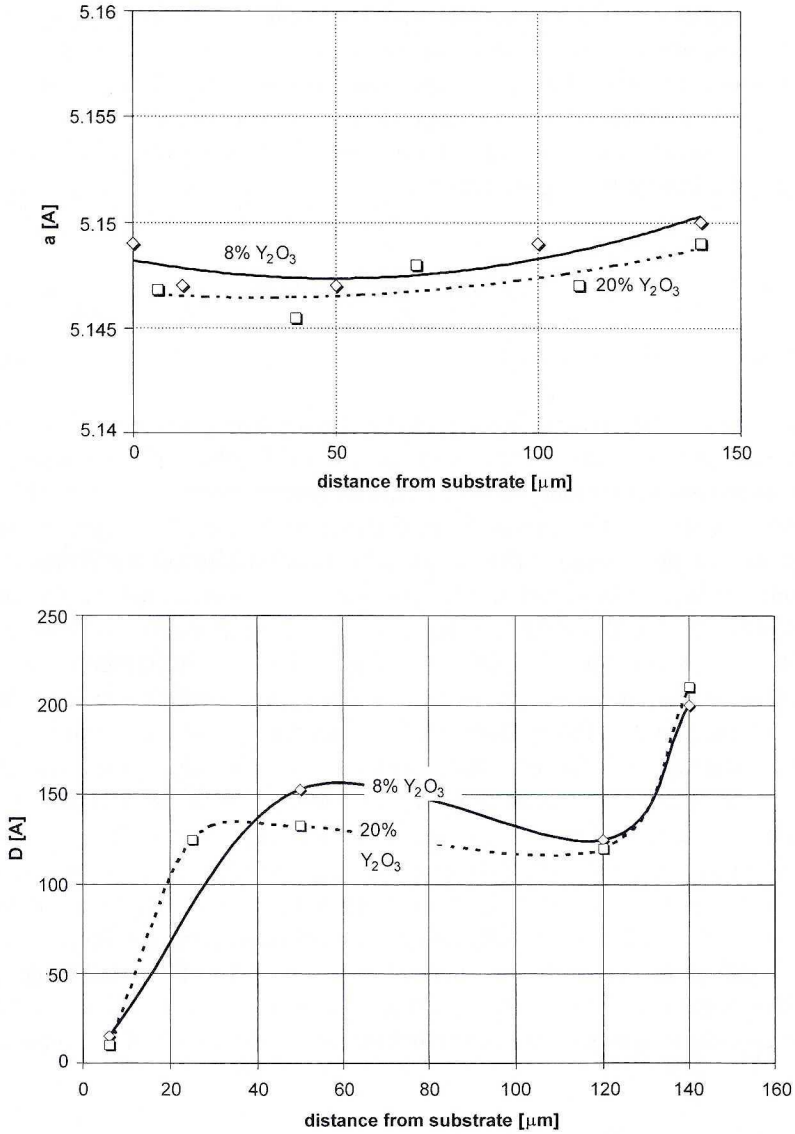


Fig. 1. The dependences of: a) the a -fcc lattice parameter on distance from the substrate and; b) crystal size, D on distance for the substrate

Fig. 3 a represents the grain structure of the 20 wt% Y_2O_3 ceramics across the layers of the coating, while Fig. 3b refers to the section cut parallel to the substrate. The structures are typical for the both alloys investigated. Layer morphology of grains of the ceramics and a smaller size in the vicinity of the transition layer can be observed in

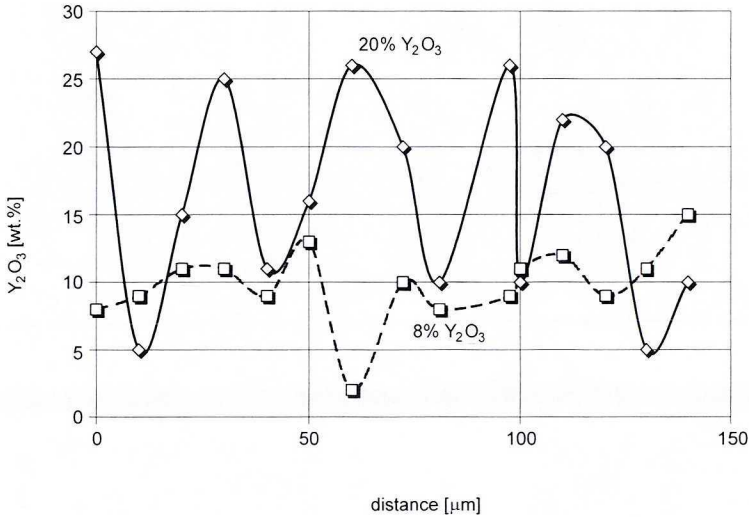


Fig. 2. The dependence of $ZrO_2 + Y_2O_3$ ceramic composition on distance from the substrate shown on the section marked A-A in Fig. 3a

Fig. 3 a. Similar arrangement of grains is also visible within the metallic plasma sprayed layer on the right hand side of Fig. 3 a.

The structure presented in Fig. 3 b, confining the morphology of the ceramics in the section parallel to the substrate near the transition layer, pictures spherical grains of 1–2 μm in diameter, which suggests the existence of columnar crystals in this area.

3.3. TEM Microstructure and chemical composition (EDS) analyses

The TEM microstructure observations were performed together with the analysis of diffraction patterns (SAED) in three places on the cross-section of the joint consisting of the metallic transition layer containing Ni, Cr, Al., Fe, Y and ceramic layer with 20 wt% Y_2O_3 :

- I. metallic transition layer close to the substrate,
- II. transition layer close to the ceramics
- III. ceramic layer close to the metallic transition layer.

Within the transition layer in area I, subgrains elongated in the direction of heat flow and about 100 nm broad were noticed. They appeared as a result of rapid solidification. The SAED shown in Fig. 4b corresponds to Ni-based phase of fcc structure, while in the SAED taken on area A rings correspond to d -lattice distances of fine crystalline NiO with cubic symmetry and tetragonal Cr_3O_4 , which originated

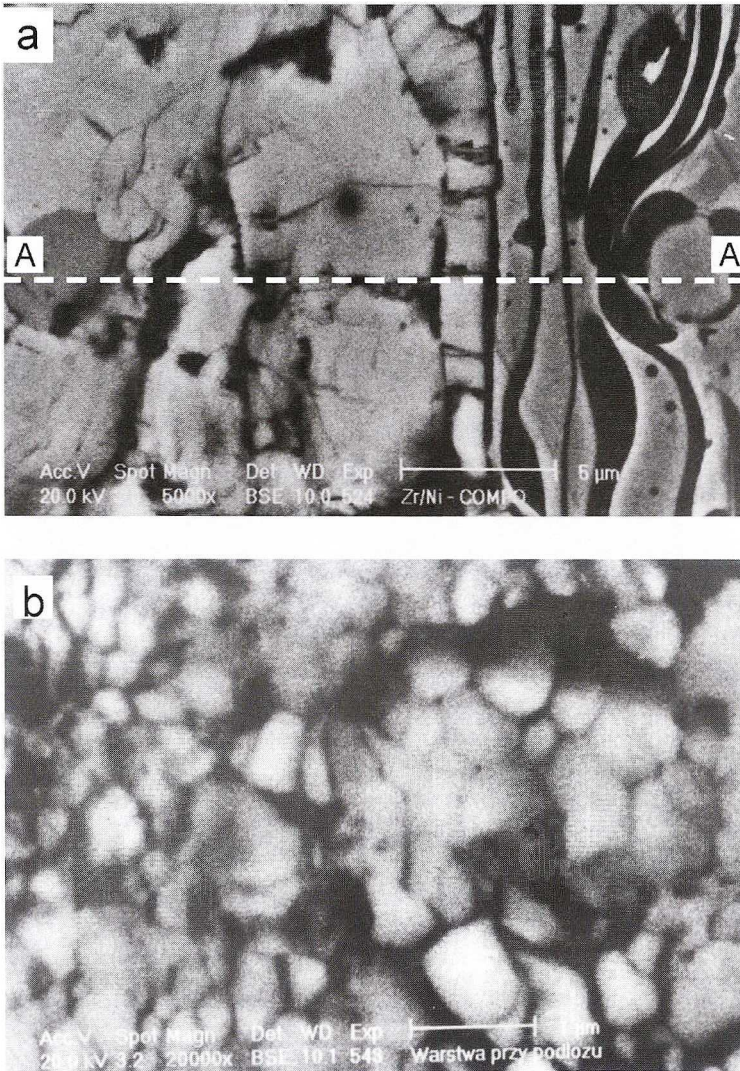


Fig. 3. SEM microstructure of $ZrO_2 + 20 \text{ wt\% } Y_2O_3$ ceramics on the section; a) perpendicular to the substrate (the metallic transition layer visible on the right side of the micrograph); b) parallel to the substrate, near the transition layer

from the deposition of metallic layer onto the substrate in the atmosphere of air plasma.

An area of elongated forms of amorphous morphology, containing fine-crystalline particles of $\gamma\text{-Al}_2O_3$, was observed within NiCrAlFeY transition layer close to the ceramics (area II), which can be seen in the SEAD (Fig. 5c) taken from area marked A in Fig 5a. Their presence can be explained by an increased content of aluminium, which segregates in the liquid NiCrAlFeY solution during solidification in air in the

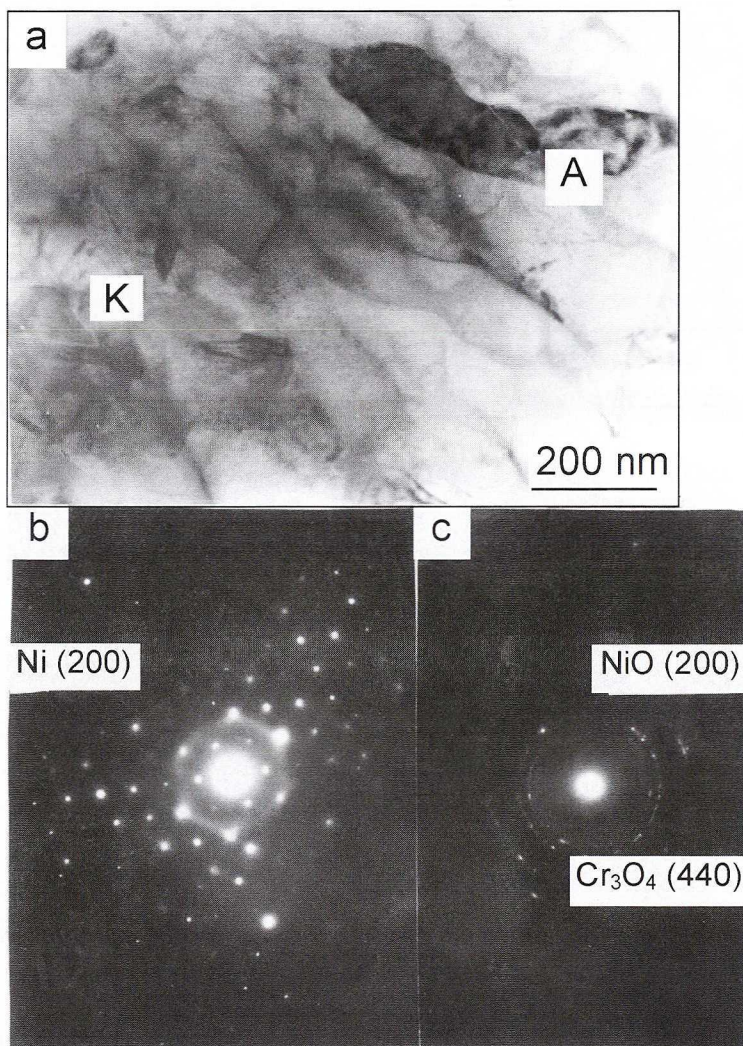


Fig. 4. a) TEM microstructure of the metallic transition layer on the boundary with the substrate; b) SAED from the area of subgrains in the centre of the micrograph; c) SAED from the area marked A

electric arc. Apart from the amorphous phases, crystalline subgrains appear with a contribution of fine-crystalline NiO particles to be seen in SAED (Fig. 5b), taken from area marked *K* in Fig. 5a.

Fig. 6a contains elongated form about 500 nm thick, which might be recognised as amorphous based on the SAED (Fig. 6c) taken of the area III, as a result of rapid solidification of the ceramic layer. Rings in the SAED correspond to fine crystalline ZrO_2 -t. The SAED, (Fig. 6b) from area *K* suggests the appearance of ZrO_2 -c with some amount of ZrO_2 -t.

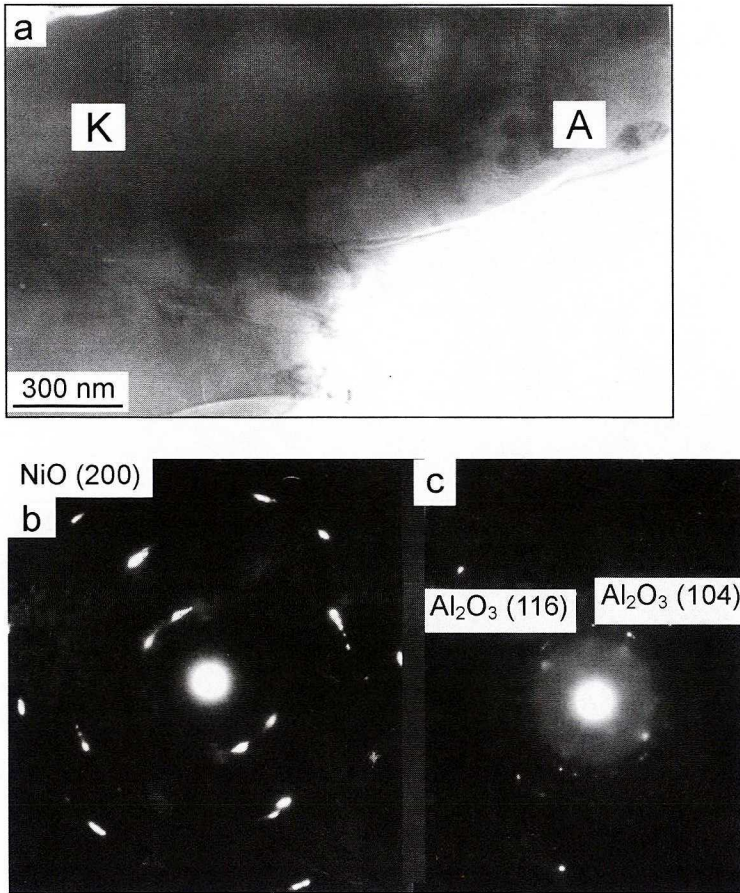


Fig. 5. a) TEM microstructure of the metallic transition layer on the boundary with the ceramics; b) SAED from the area marked K; c) SAED from the area marked A

Fig. 7 shows the changes of composition across the joint examined: ceramics (NiCrAlFeY transition layer) NiCrFe substrate performed using EDS+TEM technique. An increased amount of Ni and up to 50% of oxygen were observed in the boundary between the transition layer and the substrate. Similar amount of oxygen was detected between ceramics and transition layer accompanied by 30–40% of aluminium and 20% of chromium. The increased Al and Ni contents originate from gravity segregation. The nickel atoms seem to diffuse from the metallic layer into the transition one. The identified metals form oxides Al₂O₃ in the boundary with the ceramics and NiO and Cr₂O₃ in the boundary with the substrate. Their fine crystalline structure apart from the amorphous phase indicates that they form in the initial stage of crystallisation after plasma spraying of the transition layer.

The composition of the ceramic layer ZrO₂+2–15 wt% Y₂O₃ confirms, that there are differences in composition in dependence on the distance from the substrate, which

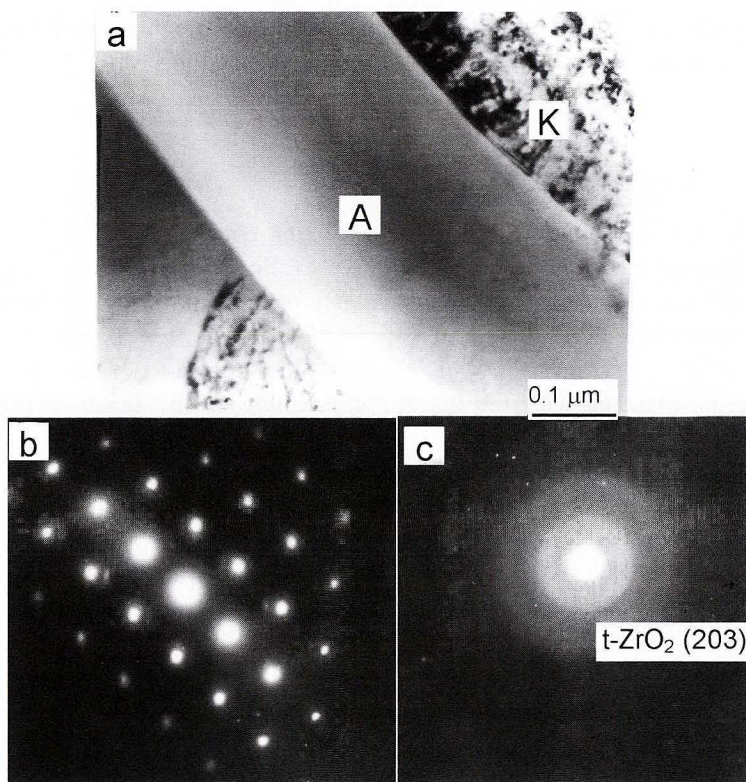


Fig. 6. a) TEM microstructure of the ceramic area near the metallic layer; b) SAED from the area on the left side of the micrograph a; c) SAED from the phase in the grain boundary

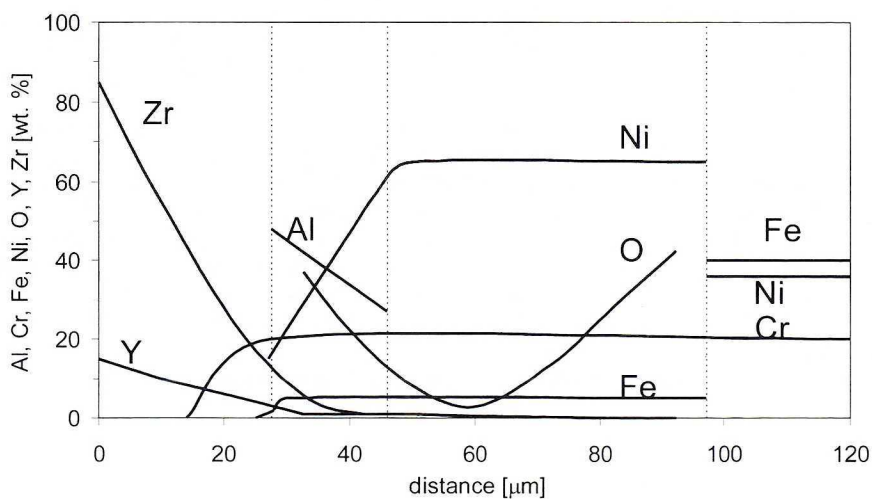


Fig. 7. The changes of the Zr and Y contents in the ceramic layer, Ni, Cr, Al, and O in the transition layer as well as Ni, Fe, Cr in the substrate

results from different solidification rates, simultaneously affecting on the occurrence of the amorphous phase in the vicinity of the air cooled metallic layer.

4. Conclusions

The performed examinations led to the following conclusions:

- The plasma spraying of transition layer followed by ceramic layer, on the Ni-based substrate results in the appearance of nonequilibrium phases due to high rates of solidification.
- The ceramic $ZrO_2 + Y_2O_3$ layer reveals the decrease of the ZrO_2 -c lattice parameter together with the size of crystallites as the distance from metallic transition layer gets smaller.
- A strong differentiation of the Y_2O_3 content within the grains of ZrO_2 -c phase has been observed due to dendritic segregation.
- The amorphous as well as fine crystalline t- ZrO_2 phase was found between the crystalline c- ZrO_2 phase layer close to the metallic transition layer of $ZrO_2 + 20$ wt% Y_2O_3 composition.
- Apart from the subgrains with fine crystalline NiO particles, the occurrence of amorphous phase with an amount of fine crystalline γ - Al_2O_3 phase particles was found in the metallic, transition layer close to the ceramics.
- The metallic transition layer near the substrate reveals elongated subgrains of Nirich fcc-phase with fine crystalline NiO and Cr_3O_4 particles.

The work was carried out within statutory research at IMMS PAS supported by State Committee for Scientific Research in co-operation with IEA, Świerk, Poland

REFERENCES

- [1] S. Stecura, *Amer. Ceram. Soc. Bull.* **56**, 1082 (1977)
- [2] T. Chreska, A.H. King, *Metal. Sci. Forum* **294–296**, 779 (1999).
- [3] C. Bartulli, L. Bertamini, S. Mtera, S. Sturlese, *Mater. Sci. and Eng.* **E 199**, 229 (1995).
- [4] W. Wołoczyński, J. Kloch, A. Pawłowski, *Bull. Acad. Pol. Sci. Ser. Techn.* **50**, 3, 181 (2002).
- [5] A. Pawłowski, T. Czeppe, L. Górski, *Metalurgia* **2**, 392–396 (2002)
- [6] L. Górski, T. Wolski, *Euro-Ceramics II*, DKG, Koln 2, 1739 (1993).
- [7] L. Górski, Report of the IAE, nr 47/A/1999.
- [8] L. Górski, A. Pawłowski, *Acta Physica Polonica* **102**, 2, 295 (2002).

REVIEWED BY: BOGUSŁAW MAJOR

Received: 27 May 2002.